Thermoresponsive Properties of *N*-Isopropylacrylamide Oligomer Brushes Grafted to Gold Nanoparticles: Effects of Molar Mass and Gold Core Size

Jun Shan,† Yiming Zhao, Niko Granqvist, and Heikki Tenhu*

Laboratory of Polymer Chemistry, Department of Chemistry, University of Helsinki, PB 55, FIN-00014 HY, Finland

Received July 11, 2008; Revised Manuscript Received February 9, 2009

ABSTRACT: To explore the thermal response of the densely packed inner regime of poly(*N*-isopropylacrylamide) (PNIPAM) brushes grafted to gold nanoparticles (AuNPs), we systematically studied the thermoresponsive properties of NIPAM oligomeric brushes affected both by oligomer molar mass and Au core size. A series of NIPAM oligomers with various molar masses ranging from ca. 600 to 3400 g/mol were obtained by RAFT polymerization and fractionated with HPLC. The AuNPs stabilized with various NIPAM oligomers were prepared by a one-pot reaction and further fractionated to achieve three pairs of AuNP fractions with narrow size distributions. When decreasing the molar mass of brush chains from ca. 3300 to 700 g/mol, a significant molar mass effect on the thermal transition was found, i.e., the phase transition temperature (defined as the endothermic peak temperature T_p by DSC) shifted from ca. 31 to 15 °C and the endothermic peak became broadened. As a comparison, we also studied the aqueous solutions of free NIPAM oligomers (molar mass from ca. 3400 to 600 g/mol) by turbidity measurements. They showed a completely opposite trend of the thermally induced phase transitions; i.e., the transition shifted to higher temperature with decreasing molar mass. The Au core size also affected the thermal response of NIPAM oligomer brushes, especially in the case of the shortest oligomers. Large Au cores caused the thermal transition of NIPAM oligomer brush to occur at lower temperatures compared to the small Au cores. This was attributed to the hydrophobic nature of Au nanocrystal surfaces. Enthalpy changes (ΔH) associated with the thermal transitions of the oligomer brushes are indicative of strong interchain interactions in the brushes, especially on large Au cores.

Introduction

Polymer brushes made of polymer chains grafted to a solid surface or interface through one end have been a subject of intensive studies in the last few decades.[1] However, polymer brushes with high grafting densities have been realized only in recent years, and are interesting because of their specific structure−property relationship.[2,3] The densely packed polymer chains avoid overlapping and thus significantly alter the conformation of individual chains in a way that they stretch away along the direction normal to the grafting surface. As a result, high-density polymer brushes can exhibit novel properties concerning their interactions with liquids, solids, nanoparticles, proteins, cells, etc.,[1−3] which are different from polymer brushes with low grafting densities. Stimuli-responsive polymer brushes are attractive owing to the change in the conformation of grafted chains in response to external stimuli which allows to construct functionalized smart surfaces.[4,5] Of the stimuli-responsive polymers, poly(*N*-isopropylacrylamide) (PNIPAM) is a well-known one which undergoes a sharp and reversible coil-to-globule phase transition at a lower critical solution temperature (LCST) of ∼32 °C in water.[6] For PNIPAM brushes, theory has predicted that thermally induced collapse depends on both grafting density and polymer molar mass, and it has also been suggested that the segment density profile exhibits the presence of a dense inner region and a dilute outer region.[7] Recent experiments have proven the validity of the predictions,[8−10] demonstrating novel properties.[11−14]

In the investigation of the core−shell structure of gold nanoparticles (AuNPs) grafted with PNIPAM (molar mass ∼5000 g/mol), we found that PNIPAM brushes with high grafting densities underwent two well-separated heat-induced phase transitions.[11] The first transition, which occurred around 31 °C, was attributed to the inner regime of PNIPAM brush with high density; the second transition, which occurred at temperatures higher than 35 °C and showed concentration dependence, was assigned to the outer regime of PNIPAM brush with a lower density.[11] Albeit similar phenomena were later reported by other groups,[13,14] for a better understanding of the thermal response of PNIPAM brushes, it is still relevant to to have a closer look into the inner regime of the brush. For this purpose, in this study, a series of NIPAM oligomers with various molar masses ranging from ca. 600 to 3400 g/mol were prepared by RAFT polymerization, followed by fractionation with HPLC. The gold nanoparticles (AuNPs) stabilized with various NIPAM oligomers were prepared in a one-pot reaction and further fractionated to achieve there pairs of AuNP fractions with large and small Au cores. We systematically studied the thermoresponsive properties of NIPAM oligomer brushes varying both the oligomer molar mass and the Au core size. As a comparison, the thermal phase transitions of the corresponding free NIPAM oligomers dissolved in water were carried out by turbidity measurements.

Experimental Section

Chemicals. *N*-Isopropylacrylamide (NIPAM, Polyscience Ins.) was recrystallized twice from benzene. Hydrogen tetrachloroaureate(III) hydrate ($HAuCl_4 \cdot xH_2O$, Au content: 52%, Fluka) and super hydride ($LiB(C_2H_5)_3H$, 1.0 M in THF, Aldrich) were used as received. 4,4′-Azobis(4-cyano-1-pentanol) as an initiator (ACP, Langfang Triple-well Chemicals Co., Ltd., China) was recrystallized from ethanol. A neutral RAFT agent with a hydroxy end group, 4-cyano-1-hydroxypent-4-yl dithiobenzoate was prepared according to the literature.[15] 2-Hydroxyethyl acrylate (HEA, Pfaltz & Bauer Inc.) was used as received. Dioxane (Laboratory-Scan, Analytical Ac.) was distilled before use. All other solvents with high quality

* Corresponding author. E-mail: heikki.tenhu@helsinki.fi.
† E-mail: jun.shan@helsinki.fi.

10.1021/ma802482e CCC: $40.75
Published on Web 03/10/2009

Table 1. First Group of NIPAM Oligomers and Corresponding NIPAM-*n*-HEAs Used in the Studies of Phase Transitions of Free Oligomers in Water

oligomer	M_n (g/mol) by MS	PDI by MS	M_n (g/mol) of oligomer[a]	NIPAM units	M_n (g/mol) of NIPAM-*n*-HEA
NIPAM-3	628	1.000	605	3	601
NIPAM-8	1209	1.004	1186	8	1182
NIPAM-13	1757	1.004	1734	13	1730
NIPAM-28[b]	3447	1.04	3424	28	3420

[a] The values of M_n of NIPAM oligomers obtained by subtracting the atomic mass of sodium from the values of M_n by MS [b] NIPAM-28 used without fractionation.

Table 2. Second Group of NIPAM Oligomers Used As Stabilizers in the Synthesis of Gold Nanoparticles

oligomer	M_n (g/mol) by MS	PDI by MS	M_n (g/mol) of oligomer[a]	M_n (g/mol) of brush chain	NIPAM units
NIPAM-5	854	1.000	831	709	5
NIPAM-10	1430	1.003	1407	1286	10
NIPAM-15	2030	1.003	2007	1887	15
NIPAM-28[b]	3447	1.04	3424	3304	28

[a] As in Table 1. [b] As in Table 1.

were used as received. The water used for all the measurements was deionized in an Elgastat UHQ-PS purification system.

Syntheses of NIPAM Oligomer Samples via RAFT Polymerization. We synthesized three samples of NIPAM oligomers with designed molar masses 600−1200 g/mol, 1000−2200 g/mol, and ca. 3000 g/mol, respectively. The synthesis details are presented in Table S1 in the Supporting Information. Here, the synthetic route for the first sample is given as an example. NIPAM monomer (0.65 mol/L), the chain transfer agent ACP-RAFT ([NIPAM]/[ACP-RAFT] = 55/1), and initiator ACP ([ACP-RAFT]/[initiator] = 15/1) were dissolved in 30 mL of dioxane. The solution was degassed with at least 5 freeze-evacuate-thaw cycles and sealed under nitrogen. RAFT polymerization took place at 70 °C for 20 h. The product was purified through silica flash column with ethyl acetate as eluent and the molar mass was measured by MALDI−TOF MS, M_n = 970 g/mol. The second sample was synthesized in a similar way but different molar ratios (see Table S1). These two polydisperse samples were further fractionated in order to obtain the NIPAM oligomer fractions with very narrow molar mass distributions (see Table 1 and Table 2). The fractionation method is depicted below. The third sample was used after RAFT polymerization without fractionation due to its relatively large molar mass, M_n = 3424 g/mol with a very narrow distribution, PDI = 1.04, determined by MALDI−TOF MS (denoted NIPAM-28 in Table 1 and Table 2, where 28 is the number of NIPAM repeating units).

Fractionation of NIPAM Oligomers. To obtain the wanted oligomeric fractions, two samples of NIPAM oligomers were fractionated with HPLC consisting of a semipreparative Nucleosil 120 Å CN (7 μm) 250 × 10 mm column, Waters 717 plus Autosampler, refractive index detector (Waters 2410) and Waters Autocollector III. The fractions were collected according to peak detection when possible, and otherwise according to retention time. The eluent was MeOH−H_2O with varying ratios depending on synthesis. Sample 1 (molar mass 600−1200 g/mol) was fractionated with 50/50 wt % MeOH/H_2O eluent and a flow rate of 2.00 mL/min. For sample 2 (molar mass 1000−2200 g/mol), the eluent used was 53/47 wt % MeOH/H_2O and the flow rate 0.80 mL/min. The injected sample concentration was 100 mg/mL for each fractionation, and the injected volumes varied from 10 to 1000 μL. The final fractions are combinations of fractions from several injections. The fractions were analyzed with MALDI−TOF mass spectrometer (see all mass spectra of oligomers in Figure S1 in the Supporting Information).

Michael Addition of NIPAM Oligomer Fractions. Four NIPAM oligomer fractions as shown in Table 1 were modified into NIPAM-*n*-HEA oligomers by first hydrolyzing the dithiobenzoate end groups of the oligomers into thiols and then by Michael addition of 2-hydroxyethyl acrylate (HEA).[16] In this way, hydrophilic end groups were produced to the oligomers. The method is described briefly. A fraction of NIPAM oligomer (20 mg) was dissolved in 10 mL of THF with stirring under nitrogen flow for 10 min. Then 5 mL of super hydride solution was injected into the solution. After the red color in solution disappeared, HEA (30 mg) was added and the reaction mixture was stirred overnight. The reaction mixture was purified through a silica flash column with ethyl acetate as an eluent, and the product was washed with methanol and analyzed by MALDI−TOF MS (see all mass spectra of NIPAM-*n*-HEAs in Figure S2).

Table 3. Characteristics of NIPAM Oligomer Protected AuNP Fractions

AuNPs	feed ratio[a]	D_{Au} (nm)[b]	NIPAM oligomer (wt %)[c]	formula of AuNPs[d]	σ (chain/nm^2)[e]
N5-AuNP-*L*	1/2	3.0 ± 0.5	40.2	$N_{182}Au_{976}$	4.5
N5-AuNP-*S*		2.6 ± 0.3	43.9	$N_{127}Au_{586}$	4.4
N10-AuNP-*L*	1/10	4.1 ± 0.6	25.3	$N_{124}Au_{2406}$	1.8
N10-AuNP-*S*		2.4 ± 0.4	49.5	$N_{69}Au_{459}$	2.8
N15-AuNP-*L*	1/10	3.2 ± 0.6	27.5	$N_{51}Au_{1289}$	1.1
N15-AuNP-*S*	1/2	2.0 ± 0.3	64.9	$N_{44}Au_{225}$	2.9
N28-AuNP-*S*	1/5	2.2 ± 0.3	76.4	$N_{60}Au_{314}$	3.1

[a] Feed ratio of the NIPAM oligomer to $HAuCl_4$ applied in the synthesis of corresponding AuNPs. [b] D_{Au}, the mean diameter of Au cores measured by HRTEM. [c] Weight loss of NIPAM oligomeric brush in TGA measurement. [d] Shape of Au cores taken as the truncated octahedron from ref 24. [e] Grafting density of NIPAM oligomeric brush (σ), calculated according to the surface areas of gold cores in ref 25.

Synthesis and Fractionation of Gold Nanoparticles. All batches of NIPAM oligomer protected AuNPs were prepared in one-pot reactions. The synthetic route and the characterization were described in detail in our previous work.[17] Table 3 presents the molar feed ratios of NIPAM oligomer and precursor $HAuCl_4$ in the synthesis of AuNPs. As an example, the synthesis of N5-AuNPs (i.e., AuNPs protected with NIPAM-5 oligomer) is briefly described. NIPAM-5 oligomer and $HAuCl_4$ (molar ratio 1:2) were dissolved in THF and kept in an ice−water bath for 30 min. N5-AuNPs were formed immediately with fast addition of an excess super hydride, and then the solution was stirred over 2 h at room temperature. The products were purified by sentrifugation (to remove possible nonprotected particles) and by ultrafiltration with Millipore membrane of MW cutoff 10000 and using ethanol as an eluent. Next, all the as-prepared AuNP batches were fractionated through precipitation into two fractions with different sizes and narrow size distributions. In a typical fractionation, in a round glass flask, 20 mL of *n*-hexane as nonsolvent was added into 4 mL of an ethanol dispersion of AuNPs. The turbid dispersion was allowed to settle overnight. Larger particles precipitated and stuck to the bottom of flask, while smaller particles still dispersed in liquid were collected. The procedure was repeated until a sufficiently narrow size distribution was obtained.

Instrumentation and Characterization. AuNPs and all oligomers were characterized by FT-IR spectra in the range of 4000−650 cm^{-1} with a Perkin-Elmer Spectrum One. ^{1}H NMR measurements were conducted with a 200 MHz Varian Gemini 2000 spectrometer. Deuterated chloroform (99.90%D, Euriso-top, France) was used as a solvent to dissolve the synthetic oligomers and AuNPs (the spectra not shown). The MALDI−TOF mass spectra of all oligomers were recorded in the reflector mode on a Bruker Microflex spectrometer. Dithranol was used as a matrix, and sodium trifloroacetate was added as a cationic agent to reduce spectral complexity.[18] AuNPs were characterized by high-resolution transmission electron microscopy (HRTEM, Philips CM200FEG) for the estimation of the size distribution and mean diameter of gold cores (all the images of AuNPs were shown in Figure S3), and by thermogravimetric analysis (TGA, Mettler Toledo TGA 850) for the information of the total amount of the oligomeric brushes and the residual gold. For more information, see ref 17.

Microcalorimetry. Microcalorimetric measurements were performed on a Precision Scanning VP-DSC (Microcal, LLC, Northampton, MA) microcalorimeter with a cell volume of 0.50721 mL at a heating rate of 0.5 °C/min in the range of 3−60 °C under elevated

Scheme 1. Structures of NIPAM Oligomers and Corresponding Michael Addition Products and Oligomeric Brush Chains

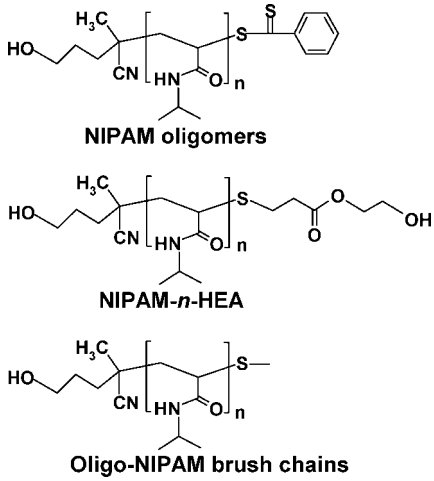

pressure (170 kPa). The sample solutions and pure deionized water as a reference were degassed by vacuum before filling into the sample cell. For each experiment, three heating scans under same conditions were normally carried out. The prescan time at 3 °C was 2 h in order to allow the collapsed NIPAM oligomeric brush chains to recover completely. All the aqueous solutions of AuNPs and oligomers, correspondingly, were filtered through Millipore filters (0.45 μm pore size) before the microcalorimetric measurements. The concentrations of the NIPAM oligomeric brushes (excluding the gold cores) were calculated.

Results and Discussion

NIPAM Oligomers. A series of NIPAM oligomer fractions with molar masses in the range of ca. 600−2000 g/mol achieved through fractionation was divided into two groups for the current studies, as shown in Tables 1 and 2. The first group in Table 1 contains three fractions and NIPAM-28, which were modified into corresponding NIPAM-*n*-HEA oligomers. The modification was considered necessary for the understanding of the thermal properties of the oligomers. The hydrophobic end groups are known to have a noticeable effect on the behavior of NIPAM polymers[19,20] and oligomers.[21−23] Therefore, the hydrophobic dithiobenzoate end groups of the original NIPAM oligomer fractions were modified into neutral hydrophilic ends of NIPAM-*n*-HEA oligomers. Scheme 1 illustrates the structures of NIPAM oligomers and corresponding NIPAM-*n*-HEAs as well as brush chains grafted to gold nanoparticles. The second group of oligomers, shown in Table 2 includes three fractions and NIPAM-28 which were applied as stabilizers in the synthesis of AuNPs. The thermoresponsive behavior of NIPAM oligomer brushes end-grafted to AuNPs in water will be compared with those of aqueous solutions of free NIPAM-*n*-HEA oligomers.

In Tables 1 and 2, the value of M_n given directly from MALDI−TOF MS includes the atomic mass of a sodium ion due to the use of sodium trifloroacetate as a cationic agent.[18] Therefore, to obtain the M_n of a NIPAM oligomer, the atomic mass of sodium was subtracted. When NIPAM oligomers were grafted to gold cores through a sulfur, a $C_6H_5-C{=}S$ was removed from each oligomeric chain. The final M_n values of the brush chains were used in the analyses of TGA and microDSC data.

Gold Nanoparticles. All batches of the NIPAM oligomer protected AuNPs were fractionated in order to get particles with narrow size distributions. Table 3 summarizes the characteristics of all the fractions of AuNPs, where, for example, N5-AuNP-*L* and -*S* mean the large and small Au cores, respectively, stabilized with a NIPAM-5 brush. We can see the following points: (i) Large and small sizes of Au cores can be obtained by either fractionating of AuNPs synthesized in one pot (such as two pairs of N5-AuNPs and N10-AuNPs) or by tuning the feed ratio between NIPAM oligomer and $HAuCl_4$ in the synthesis of AuNPs (like one pair of N15-AuNPs in Table 3). (ii) The large Au cores have more brush chains but with a bit lower grafting density in comparison to the small Au cores. This is attributed to the features of gold clusters as has been shown to be the case also with alkanethiolate protected gold clusters.[25] (iii) Though all the values of the grafting densities (σ, chains/nm^2) shown in Table 3 vary with Au core sizes, they are all above the critical value of grafting density 0.07 chains/nm^2 over which the chains are in the brush regime rather than the so-called mushroom regime.[26] Indeed, in this study all the NIPAM oligomer brushes are very dense. We can see that the fractionation of AuNPs helps to narrow the size distribution (<15% deviation for all fractions shown in Table 3) comparing to the usual value >30% before the fractionation.

Phase Transitions of Free NIPAM Oligomers in Water. Although previous studies of PNIPAM and other thermoresponsive polymers in water have shown the LCST to be independent of the molar mass, it has recently been reported that the LCST has molar-mass dependence especially for low-molar-mass PNIPAMs.[21,22] To reveal the thermal response of the very low-molar-mass NIPAM oligomers in this study, turbidity measurements on four free NIPAM oligomers (see Table 1) dissolved in water were performed, as demonstrated in Figure 1. The phase transitions of the aqueous solutions of four oligomers show strong concentration dependence. For NIPAM-28-HEA, the longest oligomer used in this study, the thermal phase transition gets sharp when increasing the concentration from 0.5 to 10.0 mg/mL, consistent with the previous reports for NIPAM oligomers with molar mass similar to NIPAM-28.[22] However, the other three shorter oligomers present gradual thermal phase transitions at different concentrations. Especially interesting, even the shortest oligomer NIPAM-3-HEA which has no recognizable transition at 10 mg/mL, undergoes a transition at higher concentrations. We can see a clear molar mass dependence of phase transition of NIPAM oligomers, i.e., with decreasing the molar mass the phase transition shifts to a higher temperature range. It would be beneficial to extend the range of experiments to higher concentrations. However, due to the very minute amounts of the samples this was not possible. So far, quite few reports have discussed the phase transition behaviors of NIPAM oligomers. Stöver group first reported the molar mass dependence of the cloud points for the low-molar-mass and narrow-disperse PNIPAMs (with no fractionation).[21,22] Kakuchi studied the thermoresponsive properties of end-functionalized NIPAM oligomers.[23] In these reports, however, the lowest molar mass of PNIPAM used was over 3000 g/mol. Here, we revealed for the first time the thermal response of a series of NIPAM oligomers with molar masses from an extremely low ca. 600 g/mol (only composed of 3 NIPAM repeating units) up to ca. 3000 g/mol. This is significant because it not only extends the range of thermoresponsive NIPAM family to as small molecules as NIPAM-3 but also gives us an opportunity to exploit such small thermoresponsive molecules to stabilize metallic nanoparticles for potential applications.

Brush Molar Mass Effect on Thermal Response. To study the brush molar mass effect on the thermal response, we chose four fractions of AuNPs from Table 2, i.e., N5-AuNP-S, N10-AuNP-S, N15-AuNP-S, and N28-AuNP-S, which have similar Au core sizes and higher grafting densities but the brush chain lengths vary. The microcalorimetric endotherms of the four aqueous dispersions of AuNPs are shown in Figure 3. The

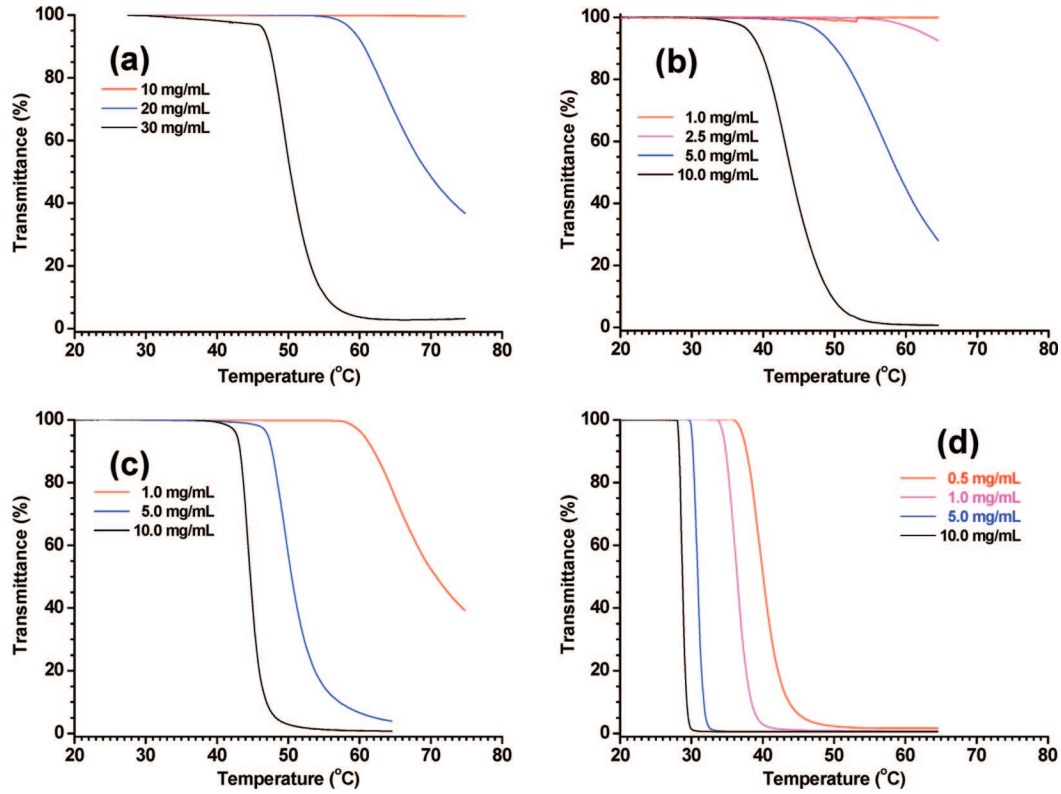

Figure 1. Turbidity measurements of four types of free NIPAM oligomers in water: (a) NIPAM-3-HEA, (b) NIPAM-8-HEA, (c) NIPAM-13-HEA, and (d) NIPAM-28-HEA.

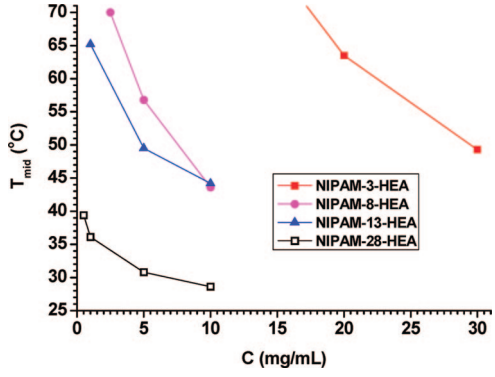

Figure 2. The transition temperature (T_{mid}) as a function of oligomer concentration (c).

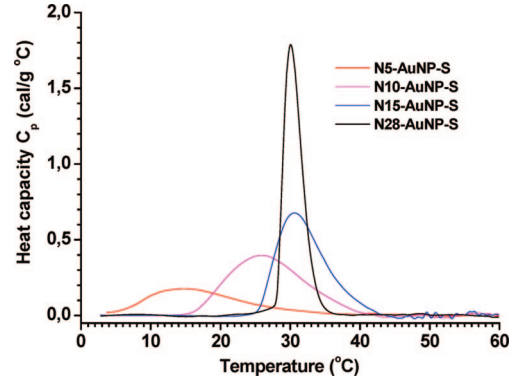

Figure 3. Brush molar mass effect on the phase transitions. Microcalorimetric endotherms of the four dispersions of N5-AuNP-*S*, N10-AuNP-*S*, N15-AuNP-*S*, and N28-AuNP-*S* in water. In each case the concentration of NIPAM oligomer brush (excluding the gold cores) is 1.0 mg/mL, with heating rate 0.5 °C/min.

thermodynamic parameters were obtained from the endotherms and are presented in Table 4. All the four oligomer brushes show thermal transitions. The most surprising feature shown in Figure 3 is that with decreasing the brush molar mass the transition temperature (say, the endothermic peak temperature T_p in Table 4) shifts from ca. 31 to 15 °C. This trend is completely opposite to that for the corresponding free NIPAM oligomers as has been shown in Figure 2. These reverse trends with decreasing the molar mass get much more visible in Figure 4 which shows the transition temperature as a function of the molar mass of NIPAM oligomers. Note that for the shortest free NIPAM-3-HEA, the value of T_{mid} is for a solution with c = 20 mg/mL, different from others corresponding to c = 5 mg/mL, because no thermal response was observed when c = 10 mg/mL (see Figure 1a). We can see that the NIPAM oligomer brushes have the transition temperatures lower than those of free oligomers until crossing/overlapping with each other at ca. 31 °C as the molar mass is ca. 3500 g/mol. We think that, comparing to the free NIPAM oligomers in water, the brush chains favor to interact through H-bonding with each others,

Table 4. Thermodynamic Parameters Calculated from Microcalorimetric Endotherms of Aqueous Dispersions of AuNPs

AuNP	T_p (°C)	T_{onset} (°C)	$\Delta T_{1/2}$ (°C)	ΔH (kJ/mol)
N5-AuNP-*L*	11.7	<3	13.5	1.05
N5-AuNP-*S*	15.0	6.0	14.4	2.23
N10-AuNP-*L*	21.8	15.0	8.7	1.35
N10-AuNP-*S*	26.0	16.0	13.0	2.49
N15-AuNP-*L*	29.3	20.5	7.6	0.73
N15-AuNP-*S*	30.6	25.5	7.6	2.66
N28-AuNP-*S*	30.5	28.0	3.3	3.57

rather than with water molecules, due to the high grafting densities.[9,10] This interaction makes the thermal response occur earlier at a low temperature. With decreasing the brush molar mass, the chains are expected to be more stretched with restricted freedom within a small conic space close to the curved surface

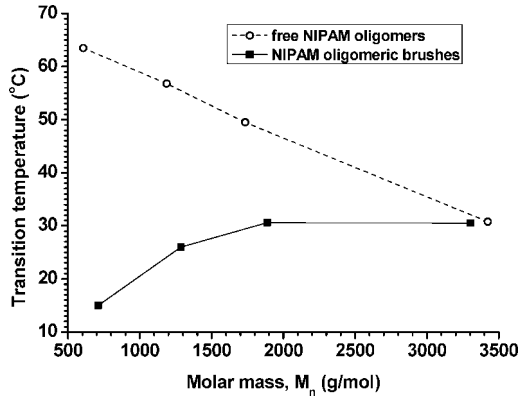

Figure 4. The thermoresponsive transition temperature as a function of the molar mass of NIPAM oligomers for both free NIPAM oligomers and NIPAM oligomeric brushes in water. Notes: (1) for the free NIPAM oligomers, the values of T_{mid} were used as the transition temperatures at $c = 20$ mg/mL for NIPAM-3-HEA, and $c = 5$ mg/mL for other three oligomers; (2) for NIPAM oligomeric brushes, the values of T_p were plotted as the transition temperatures as shown in Table 4.

of nanoparticles, reinforcing the interchain interaction and leading to an earlier transition.[11]

Another impressive feature revealed in Figure 3 is the broadening of transition with decreasing molar mass. The width of the endothermic peaks for the four AuNPs (see $\Delta T_{1/2}$ in Table 4), with decreasing the brush molar mass, increases markedly from ca. 3 to 15 °C. Meanwhile, the thermal transition starts at a very low temperature (see T_{onset} in Table 4). The broadening of the transition will be discussed in the next subsection together with the Au core size effect.

Gold Core Size Effect on Thermal Response. It is known that the properties of polymeric brushes are affected by substrates, e.g., the glass transition temperature of the brushes, in particular for low-molar-mass polymers.[2] What about the impact of the gold nanocrystals on the thermoresponsive properties of PNIPAM brushes? To study this effect, we chose three pairs of the AuNP fractions stabilized with various NIPAM oligomers. Each pair includes two fractions, one with a relatively large core and another with a small core (see Table 3). It is worth noting that the grafting density varies with the core size due to the synthesis method applied to prepare AuNPs in this study, i.e, the large cores have a low grafting density, while the small cores have high density.[27] The Au core size effect on thermal transition was investigated with microcalorimetry as shown in Figure 5. It can be seen that the thermal transition shifts when changing the size of the core. On the average, the differences in the particle sizes are very small. However, the size distributions are different and this clearly affects the thermal beahvior of the oligomers. For large AuNPs the thermal transition occurs at a lower temperature range than that for small AuNPs. Comparing the thermograms of three pairs, we found that the shifts of the transition gaps for two pairs of N5-AuNP-*L*/-*S* and N10-AuNP-*L*/-*S* are large, but gets smaller for N15-AuNP-*L*/-*S*. Therefore, we can conclude that (i) the Au core size has a noticeable effect on the thermal transition of the shorter NIPAM oligomer brushes; (ii) as the brush molar mass increases, say over 2000 g/mol, the effect becomes less pronounced; (iii) the large Au cores cause an earlier thermal transition of NIPAM oligomer brush, and *vice versa*.

It is generally assumed that gold nanocrystals larger than 0.8 nm have a truncated octahedral or cuboctahedral shape, depending on the number of gold atoms in the core, with eight {111} facets truncated by six smaller {100} facets.[28] It is known that the Au{111} surface in water exhibits hydrophobic behavior.[29,30] Therefore, it is reasonable to assume that overall the Au

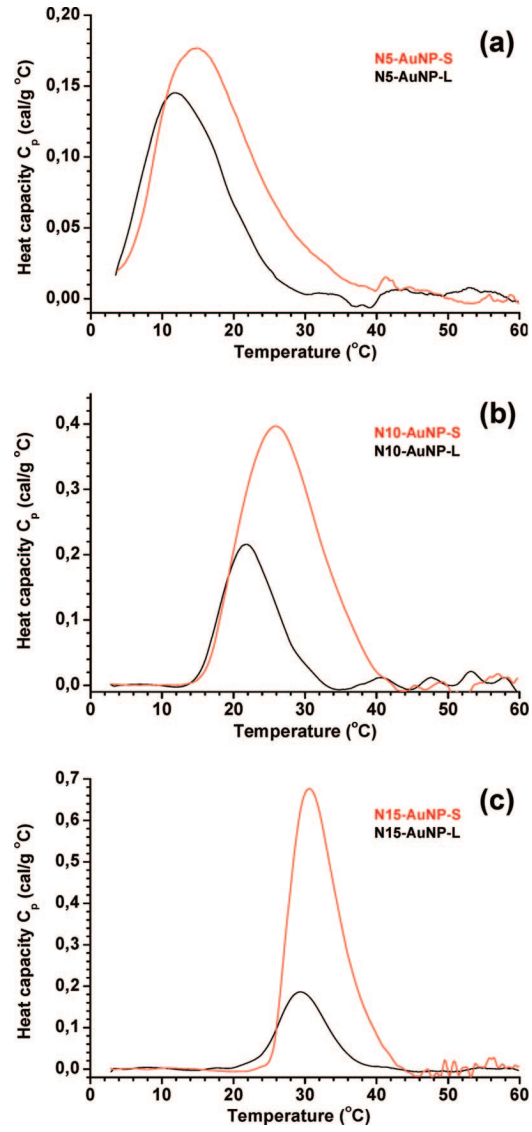

Figure 5. Gold core size effect on the thermal transitions. Microcalorimetric endotherms of the dispersions of (a) N5-AuNP-*S* and N5-AuNP-*L*, (b) N10-AuNP-*S* and N10-AuNP-*L*, and (c) N15-AuNP-*S* and N15-AuNP-*L* in water. Each concentration of NIPAM oligomeric brush (excluding the gold cores) is 1.0 mg/mL, with heating rate 0.5 °C/min.

nanocrystal surfaces are to some extent hydrophobic, even though this basic question still remains open. Hence, a gold nanocrystal stabilized with NIPAM oligomer brush can be seen as an analogue of an amphiphilic star copolymer, where the oligomer brush chains are the hydrophilic arms and the Au nanocrystal is like hydrophobic polymers as a core. As a consequence, the Au core size effect on thermoresponsive properties can be attributed to the hydrophobicity of Au cores. We may expect the thermal behavior resembling that of amphiphilic PNIPAMs.[20] The large hydrophobic Au cores would prohibit water molecules to penetrate into the dense NIPAM oligomer brushes and impede the interaction between the oligomer chains and water molecules. Thus, interchain interaction would increase, this resulting in an earlier thermal transition of NIPAM oligomer brushes. This speculation agrees well with the enthalpy changes (ΔH) in the course of thermal transition of NIPAM oligomer brushes estimated from microcalorimetry, which detects the disruption of the hydrogen bonds among the amide groups and water molecules during the transition.[31] All the ΔH values are summarized in Table 4. We can see that for the large particles the ΔH value is always smaller than that

for the small particles in each pair of AuNPs. The different ΔH values in each pair of AuNPs also suggest that stronger interchain interaction exist in the brushes on large Au cores than in the brushes on small Au cores. This conclusion is in good agreement with the fact that the majority of large Au core surfaces is composed of the Au{111} facets rather than edges and corners, leading to "bundles" of ordered chains with gaps (areas with a disordered organic layer) at the corners and vertexes.[28,32] Corbierre et al.[33] suggested that for polymeric brushes on Au cores there are voids at the facet edges and the percentage of void volume greatly decreases with increasing Au core diameter in the range of ca. 1−5 nm with various brush thicknesses. The sizes of the gold cores studied in this paper are within this range.

The broadening of the thermal response of NIPAM oligomer brushes as revealed in Figures 3 and 4 agree with the theoretical predictions[7] and experiments[12] reported on the phase transition of PNIPAM brushes on flat surfaces with a high grafting density. This is due to the fact that the response of a brush is associated with conformational changes of grafted chains via segmental diffusion,[3] and therefore at a high grafting density the interchain interaction and the local viscosity of the brush can be very high, likely resulting in a slow response. On the other hand, that the broadness of the endothermic peak becomes noticeably wider with decreasing the brush molar mass is indicative of the effect resulted from the gold core, to some extent because of the hydrophobicity of the gold cores.

Conclusions

We synthesized NIPAM oligomers by RAFT polymerization and successfully fractionated them by HPLC. We obtained a series of NIPAM oligomer fractions with various molar masses ranging from ca. 600 to 3400 g/mol. We then prepared gold nanoparticles stabilized with various NIPAM oligomer fractions and further fractionated them to achieve fractions of gold nanoparticles with different sizes and narrow size distributions. By microcalorimetry, the brush molar mass effect and the Au core size effect on the thermoresponsive properties of NIPAM oligomeric brushes in water were investigated. As a comparison to the oligomeric brushes, the turbidity measurements on the aqueous solutions of corresponding free NIPAM oligomers were also carried out. A significant effect of the brush molar mass on the thermal transition was found, which is completely opposite to that for the corresponding free NIPAM oligomers. The Au core size affects the transition temperature not as significant as the brush molar mass, but causes a slow transition behavior due to the high interchain interaction and the hydrophobic nature of Au nanocrystal surfaces.

Acknowledgment. We are grateful to Prof. Søren Hvidt, University of Roskilde, Denmark, for suggestions for fractionation of NIPAM oligomers. We also thank Prof. Françoise Winnik, Université de Montréal, for valuable discussion. Dr. Hua Jiang and Prof Janne Ruokolainen, Helsinki University of Technology, are thanked for TEM images.

Supporting Information Available: A table of synthesis data and figures showing MALDI−TOF mass spectra and TEM images and plots of size distributions. This material is available free of charge via the Internet at http://pubs.acs.org.

References and Notes

(1) *Polymer Brushes: Synthesis, Characterization, Applications*; Advincula, R. C.; Brittain, W. J.; Caster, K. C.; RüheJ., Ed.; Wiley-VCH: Weinheim, Germany, 2004.
(2) Tsujii, Y.; Ohno, K.; Yamamoto, S.; Goto, A.; Fukuda, T. *Adv. Polym. Sci.*, **2006**, *197*, 1−45.
(3) Brittain, W. J.; Minko, S. *J. Polym. Sci., Part A: Polym. Chem.* **2007**, *45*, 3505–3512.
(4) Kaholak, M.; Lee, W-K.; LaMattina, B.; Caster, K. C.; Zauscher, S. Polymerization, Nanopatterning and Characterization of Surface-Confined, Stimulus-Responsive Polymer BrushesIn ref 1, pp 381−402.
(5) Brittain, W. J.; Boyes, S. G.; Granville, A. M.; Baum, M.; Mirous, B. K.; Akgun, B.; Zhao, B.; Blickle, C.; Foster, M. D. *Adv. Polym. Sci.*, **2006**, *198*, 125−147.
(6) Aseyev, V. O.; Tenhu, H.; Winnik, F. M. *Adv. Polym. Sci.* **2006**, *196*, 1–85.
(7) Borisov, O. V; Zhulina, E. B. *Responsive polymer Brushes: A Theoretical Outlook. In Smart Polymers: Applications in Biotechnology and Biomedicine*, 2nd ed.; Galaev, I.; Mattiasson, B., Eds.; CRC Press: Boca Raton, FL, 2008.
(8) Yim, H.; Kent, M. S.; Satija, S.; Mendez, S.; Balamurugan, S. S.; Balamurugan, S.; Lopez, G. P. *Phys. Rev. E* **2005**, *72*, 051801.
(9) Plunkett, K.; Zhu, X.; Moore, J. S.; Leckband, D. E. *Langmuir* **2006**, *22*, 4259–4266.
(10) Yim, H.; Kent, M. S.; Mendez, S.; Lopez, G. P.; Satija, S.; Seo, Y. *Macromolecules* **2006**, *39*, 3420–3426.
(11) Shan, J.; Chen, J.; Nuopponen, M.; Tenhu, H. *Langmuir* **2004**, *20*, 4671–4676.
(12) Balamurugan, S.; Mendez, Sergio; Balamurugan, S. S.; O'Brien II, M. J.; Lopez, G. P. *Langmuir* **2003**, *19*, 2545–2549.
(13) Xu, J.; Luo, S.; Shi, W. *Langmuir* **2006**, *22*, 989–997.
(14) Luo, S.; Xu, J.; Zhu, Z.; Wu, C.; Liu, S. *J. Phys. Chem. B* **2006**, *110*, 9132–9139.
(15) Thang, S. H.; Chong, Y. K.; Mayadunne, R. T. A.; Moad, G.; Rizzardo, E. *Tetrahedron Lett.* **1999**, *40*, 2435–2438.
(16) Qiu, X.-P.; Winnik, F. M. *Macromol. Rapid Commun.* **2006**, *27*, 1648–1653.
(17) Shan, J.; Nuopponen, M.; Jiang, H.; Kauppinen, E.; Tenhu, H. *Macromolecules* **2003**, *36*, 4526–4533.
(18) Favier, A.; Ladavière, C.; Charreyre, M.-T.; Pichot, C. *Macromolecules* **2004**, *37*, 2026–2034.
(19) Furyk, S.; Zhang, Y.; Ortiz-Acosta, D.; Cremer, P. S.; Bergbreiter, D. E. *J. Polym. Sci., Part A: Polym. Chem.* **2006**, *44*, 1492–1501.
(20) Kujawa, P.; Segui, F.; Shaban, S.; Diab, C.; Okada, Y.; Tanaka, T.; Winnik, F. M. *Macromolecules* **2006**, *39*, 341–348.
(21) Xia, Y.; Yin, X.; Burke, N. A. D.; Stöver, H. D. H. *Macromolecules* **2005**, *38*, 5937–5943.
(22) Xia, Y.; Burke, N. A. D.; Stöver, H. D. H. *Macromolecules* **2006**, *39*, 2275–2283.
(23) Duan, Q.; Miura, Y.; Narumi, A.; Shen, A.; Sato, S.-I.; Satoh, T.; Kakuchi, T. *J. Polym. Sci., Part A: Polym. Chem.* **2006**, *44*, 1117–1124.
(24) Whetten, R. L.; Shafigullin, M. N.; Khoury, J. T.; Schaaff, T. G.; Vezmar, I.; Alvarez, M. M.; Wilkinson, A. *Acc. Chem. Res.* **1999**, *32*, 397–406.
(25) Hostetler, M. J.; Wingate, J. E.; Zhong, C.-Z.; Harris, J. E.; Vachet, R. W.; Clark, M. R.; Londono, J. D.; Green, S. J.; Stokes, J. J.; Wignall, G. D.; Glish, G. L.; Porter, M. D.; Evans, N. D.; Murray, R. W. *Langmuir* **1998**, *14*, 17–30.
(26) Wu, T.; Efimenko, K.; Genzer, J. *J. Am. Chem. Soc.* **2002**, *124*, 9394.
(27) Shan, J.; Tenhu, H. *Chem. Commun.* **2007**, 4580–4598.
(28) Love, J. C.; Estroff, L. A.; Kriebel, J. K.; Nuzzo, R. G.; Whitesides, G. M. *Chem. Rev.* **2005**, *105*, 1103–1169.
(29) Smith, R. S.; Huang, C.; Wong, E. K. L.; Kay, B. D. *Surf. Sci.* **1996**, *367*, L13–L18.
(30) Meng, S.; Kaxiras, E.; Zhang, Z. *J. Chem. Phys.* **2007**, *127*, 244710.
(31) Nichifor, M.; Zhu, X. X. *Polymer* **2003**, *44*, 3053–3060.
(32) Luedtke, W. D.; Landman, U. *J. Phys. Chem. B* **1998**, *102*, 6566.
(33) Corbierre, M. K.; Cameron, N. S.; Lennox, R. B. *Langmuir* **2004**, *20*, 2867–2873.

MA802482E